INTERCOMPARISON OF NUMERICAL TECHNIQUES FOR THE SIMULATION OF VISIBILITY IMPROVEMENTS FROM SO_2 EMISSION CONTROLS IN THE EASTERN UNITED STATES

Paolo Zannetti and Ivar Tombach
AeroVironment Inc.
825 Myrtle Avenue
Monrovia, CA 91016

Abstract

Several analysts, using various analytical approaches, in recent years have estimated the visibility improvements that might result from strategies to reduce the emissions of SO_2 in the East. In particular, we developed a semiempirical analysis method to estimate visibility benefits of SO_2 emissions controls. As an example of its application, the method was used to estimate visual range improvements from the control of 12 million tons per year of SO_2 emissions in 31 eastern states. Others have performed similar analyses using different approaches, specifically simulation modeling and a transfer matrix approach based on regional simulation modeling. In order to understand better the significance of the results from these analyses, which have used different meteorological inputs and assumptions, we compared these three methods under comparable input conditions and assumptions. We found many aspects of agreement and some significant differences.

Introduction and Overview

Fine particles, i.e., particles whose aerodynamic diameters are less than 2.5 μm, are the most effective atmospheric component for visibility degradation. A large fraction of fine particles can be sulfate-containing particles, which are generated predominantly by atmospheric chemical reactions that oxidize the gaseous SO_2, mostly emitted from anthropogenic sources, into sulfate particles (SO_4^{2-}).

Several studies have employed regional models in an attempt to quantify the role of SO_2 emission reduction scenarios. Models have been used directly to calculate effects of emission changes[1,2], or benefits of controls have been inferred by varying the predictions of a single simulation, using a transfer matrix approach.[3] Such quantifications, however, are difficult to perform for several reasons: 1) the large uncertainties that even advanced models possess in simulating long-range transport, diffusion, chemistry and deposition of atmospheric sulfur; 2) the difficulty in quantifying the roles that other components, such as non-sulfate-containing fine particles, coarse particles and gases, play in visibility impairment; and 3) the scarcity of suitable field data for inputs.

In an effort to better illuminate the processes involved in the relationship between emission changes and visibility changes, AeroVironment Inc. (AV) developed an approach that came to be known as a "semiempirical analysis" approach.[4,5]

From "Visibility and Fine Particles," a Transactions of the
Air & Waste Management Association edited by C. V. Mathai (1990)

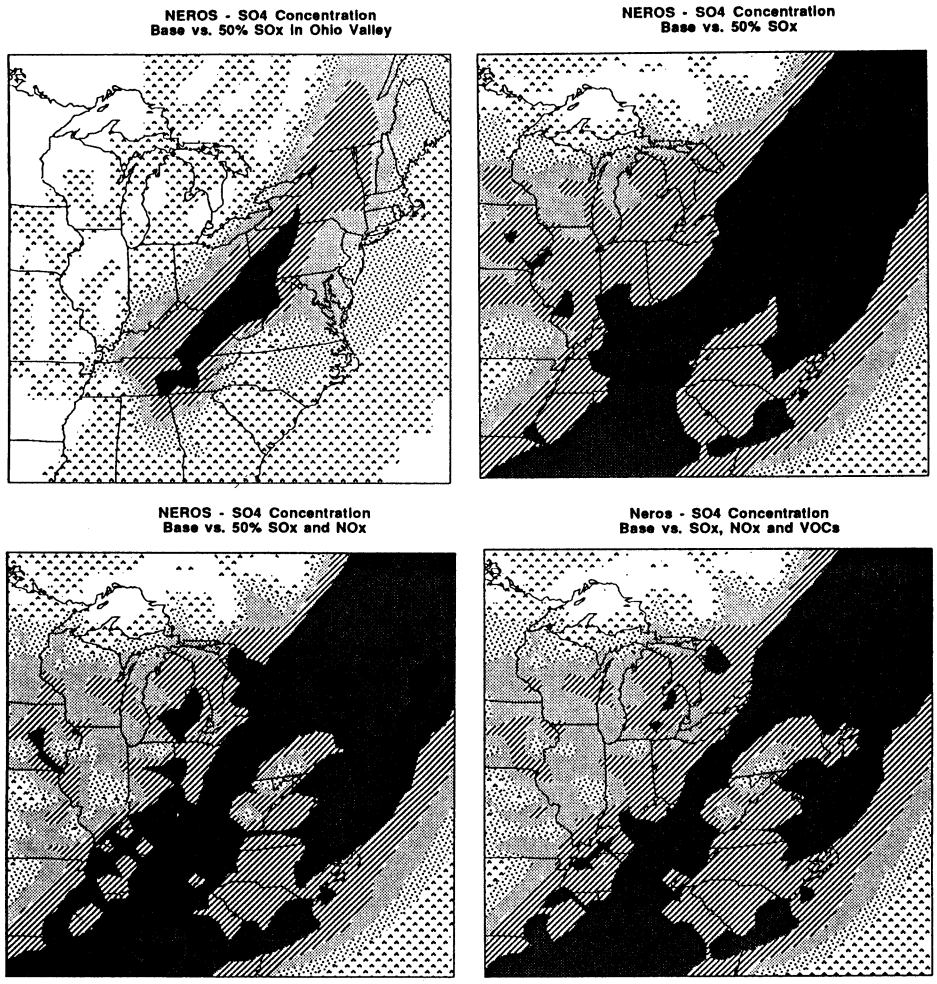

Figure 3. Comparisons of the NEROS 65 GMT surface level sulfate concentrations for the base case and the 50% SOx reduction in the Ohio River Valley case (3a), the 50% SOx reduction over the entire domain case (3b), the 50% SOx and NOx reduction case (3c) and the 50% SOx, NOx and VOC reduction case (3d) are expressed as (perturbation case-base case) / base case.

The results of applications of these three methods are not wholly consistent with each other, but it was not clear whether the differences reflect intrinsic differences in the methods or just that they were applied to situations that are not comparable, with differing meteorological inputs and assumptions. In order to understand the differences, we undertook, with the cooperation of individuals who had done the previous modeling and transfer matrix simulations, to compare the methods under similar input assumptions.

Thus, this paper presents an intercomparison of three methods that have been used to quantify the improvements in visual range that could be expected in the eastern United States from SO_2 emissions controls. These methods are

1. a semiempirical approach
2. the transfer matrix method based upon RELMAP simulations
3. the RIVAD model

The three methods are summarized first and the intercomparison results thereafter.

The Semiempirical Approach

Under the semiempirical method, the algorithm we developed[4,5] for computing each visibility improvement in a region j for a certain meteorological regime k is based on an intuitive "fractional" approach that can be described by the following points:

1. Atmospheric light extinction is due to the concentration of fine particles and other components. SO_2 emission controls will affect only the part of the fraction of light extinction that is due to fine particles.
2. Fine particles are composed of fine sulfate-containing particles and particles containing other species (but no sulfates). SO_2 emission controls will affect only the fraction of fine particles that contain sulfates.
3. Fine sulfate-containing particles are a fraction of the total concentration of sulfur in the atmosphere in both gaseous and particulate form. They are mostly produced by SO_2-to-SO_4^{2-} chemical transformations that may be nonlinear, i.e., because of the effects of time and of other reactants on the conversion, a given percentage change in SO_2 concentration may not correspond to the same percentage change in SO_4^{2-} concentration. Therefore, although SO_2 emission controls will proportionately decrease the total ambient sulfur, the fine sulfates concentrations may decrease to a lesser extent because of the nonlinear chemistry.
4. Total ambient sulfur in one geographical area is due to the sum of local SO_2 emissions and transported SO_2 from other regions. SO_2 emission controls will affect only the fraction of sulfur that is transported from the regions affected by the control scenario.

In mathematical notation, the above reasoning can be expressed as:

$$\frac{(\Delta LE)_{jk}}{(LE)_{jk}} = \alpha_{jk}\,\beta_{jk}\,\gamma_{jk}^{(w)}\,\delta_{jk}^{(w)}\frac{\Delta E}{E} \qquad (1)$$

where $(\Delta LE)_{jk}/(LE)_{jk}$ is the fractional improvement in atmospheric light extinction expected from the total fractional SO_2 emission control $\Delta E/E$, and α, β, $\gamma^{(w)}$ and $\delta^{(w)}$ are the fractions representing sulfur transport efficiency, nonlinearity of the SO_2-to-SO_4^{2-} transformation, the sulfate fraction of fine particles, and the fraction of light extinction that is attributable to fine particles, respectively. Later in this paper, the product $\gamma_{jk}^{(w)}\,\delta_{jk}^{(w)}$ will be

referred to as $\epsilon_{jk}^{(w)}$. The superscript (w) indicates that the role of water is explicitly taken into account by this methodology. (For this intercomparison, $\Delta E/E$ was chosen equal to -0.55, i.e., corresponding to a 12-million-ton-per-year reduction of eastern U.S. SO_2 emissions.)

The above calculation of light extinction improvements (which are negative numbers) can be easily related to equivalent improvements of average visual range VR (positive numbers) by the simple analytical transformation

$$I_{jk} = \frac{(\Delta VR)_{jk}}{(VR)_{jk}} = -\frac{1}{1+\frac{(LE)_{jk}}{(\Delta LE)_{jk}}}. \tag{2}$$

Then, in each region j, the annual average visual range improvements I_j are

$$I_j = \sum_k p_{jk}\, I_{jk} \tag{3}$$

where p_{jk} is the relative frequency of occurrence of the meteorological regime k in the region j.

The Transfer Matrix Approach

The transfer matrix approach has been used by the EPA[3,6] to quantify, in a relatively simple and linear form, the relationship between long-term average SO_2 emissions and air quality indicators such as ambient sulfate concentrations and total sulfur deposition. One specific application was the Regulatory Impact Analysis (RIA) for the National Ambient Air Quality Standards for SO_2.[3] Various regional dispersion models have been used with the transfer matrices.

In this comparison we focus on the transfer matrices (TM) that were computed by the EPA using calculations made by the RELMAP model (Regional Lagrangian Model of Air Pollution), a mass-conserving Lagrangian puff model that simulates ambient concentrations and wet and dry deposition of SO_2, SO_4^{2-}, and fine and coarse particulate matter over the eastern United States and southeastern Canada. These annual average TM were available for the year 1980 and for six pollution indicators: (1) SO_2 concentration, (2) SO_4^{2-} concentration, (3) SO_2 dry deposition, (4) SO_4^{2-} dry deposition, (5) SO_2 wet deposition, and (6) SO_4^{2-} wet deposition.

In mathematical notation, the transfer matrix concept can be described by the equation

$$P_m = \sum_n T_{mn}\, E_n \tag{4}$$

where P_m is one of the six pollution indicators described above and refers to the air quality impact in the cell m ($m = 1, 2, \ldots, 1350$); T_{mn} is the corresponding transfer matrix; and E_n is the SO_2 emission rate in the cell n ($n = 1, 2, \ldots, 1350$). In other words, the air quality impact P_m is assumed to be a linear combination of all the SO_2 emissions in the cells. Therefore, if the emissions E_n are reduced by ΔE_n, the air pollution indicator P_m will be reduced by ΔP_m, where

$$\Delta P_m = \sum_n T_{mn}\, \Delta E_n. \tag{5}$$

Implicit in Equation 5 is the assumption that the chemical transformation processes are "linear," i.e., they are not affected by changes in the concentration of SO_2. (Actually, Equation 5 is regorously valid only for the three SO_2 pollution indicators. To be valid for the three SO_4^{2-} pollution indicators also, we must assume that primary sulfate emissions in each cell n are reduced by the same fraction as the SO_2 emissions (i.e., $\Delta E_n/E_n$). However, even when this further assumption is not met, Equation 5 still remains applicable to the three SO_4^{2-} pollution indicators, since primary sulfate emissions are typically two orders of magnitude lower than SO_2 emissions and, therefore, their regional effects are mostly negligible.)

Transfer matrices can be used to calculate the fractional improvements of sulfate concentration in each region j. This improvement, which we denote by $[\overline{\Delta SO_4/SO_4}]_j^{REL}$ (where the superscript REL indicates results obtained from the transfer matrix approach using the RELMAP model), can be written as (using notation parallel to that of Equation 1):

$$\left[\overline{\frac{\Delta SO_4}{SO_4}}\right]_j^{REL} = \bar{\alpha}_j^{REL}\,\bar{\beta}_j^{REL}\,\frac{\Delta E}{E} = \bar{\alpha}_j^{REL}\,\frac{\Delta E}{E}. \qquad (6)$$

This simplification in the last term results because, in the transfer matrix approach, the nonlinearity coefficient β is always taken equal to one. Equation 6 allows, a "bulk" comparison between the $\bar{\alpha}_j^{REL}$ terms above, and those (α_{jk}) calculated using the AV's semiempirical approach. This is a "bulk" comparison, since only the set $[\alpha_{j1}, \alpha_{j2}, \ldots, \alpha_{j7}]$, for each region j, and not the individual α_{jk} values, can be compared.

The RIA also used other models besides RELMAP. Even though we did not obtain the original transfer matrices used in the RIA, the results in the RIA allow an approximate calculation of the corresponding α values for these other model applications.

The outputs of transfer matrix calculations of improvements in ambient sulfate concentrations were used in the RIA to calculate visibility benefits using the method described by Bachmann[7]. This method can be related to the semiempirical approach as follows.

According to the semiempirical approach, we have

$$\frac{(\Delta LE)_{jk}}{(LE)_{jk}} = \gamma_{jk}^{(w)}\,\delta_{jk}^{(w)}\,\frac{(\Delta SO_4)_{jk}}{(SO_4)_{jk}} = \epsilon_{jk}^{(w)}\,\frac{(\Delta SO_4)_{jk}}{(SO_4)_{jk}} \qquad (7)$$

which relates the fractional improvements in light extinction (LE) to the fractional improvements of the concentration of fine sulfates. The products $\epsilon_{jk}^{(w)} = \gamma_{jk}^{(w)}\,\delta_{jk}^{(w)}$ are computed for each region j and each meteorological regime k. These products will be referred to below as $\epsilon_{jk}^{(AV)}$.

The RIA used a simplified approach based on the following equation

$$\frac{\Delta VR}{VR} = \frac{N+1}{N+1+(\Delta LE_s/LE_s)} - 1 \qquad (8)$$

where $\Delta VR/VR$ is the fractional improvement in visual range, N is equal to LE_{ns}/LE_s, LE_s is the "initial" (i.e., before the SO_2 emission controls) light extinction due to fine sulfates, LE_{ns} is the initial light extinction due to nonsulfate (i.e., everything else), and $\Delta LE_s/LE_s$ is the fractional improvement of the sulfate contribution to light extinction, a term that can be

assumed to be equal to the fractional improvement in sulfate concentration $\Delta SO_4/SO_4$, if the sulfate light extinction efficiency does not change with time.

By substitution of the above terms into Equation 8 and by using the relationship of Equation 2 between visual range (VR) and light extinction (LE) improvements, we obtain

$$\frac{\Delta LE}{LE} = \frac{1}{1+N} \frac{\Delta SO_4}{SO_4} \tag{9}$$

and, therefore,

$$\epsilon_{jk}^{(w)} = \frac{1}{1+N} \tag{10}$$

for every j and k. Equation 10 correctly gives, for N = 0 (i.e., all light extinction due to sulfate particles), $\epsilon^{(w)} = 1$, while, for $N = \infty$ (i.e., no light extinction due to sulfate particles), $\epsilon^{(w)} = 0$.

Equation 10 shows that the transfer matrix approach, as used in the RIA, implies a constant $\epsilon^{(w)}$. Bachmann[7] recommended a range of N = 1.0 to 1.5 for annual average changes and the RIA actually used N = 1.25, which gives $\epsilon^{(w)} = 0.44$, a value that we will refer to as ϵ^{TM}.

The RIVAD Model

The RIVAD model has been used by Systems Applications, Inc. (SAI) for assessments of the potential visibility benefits of SO_2 controls, initially as part of a report for the EPA[1] and then as the basis for a later analysis.[2] For this intercomparison, AV collaborated with SAI, who reran the RIVAD model for the entire year 1980 and saved the daily (noontime) outputs of ambient SO_2 and SO_4^{2-} concentrations over each 80 km x 80 km cell covering the eastern United States. These daily outputs allowed the calculation of not only annual average improvements, but also sulfate and visual range improvements for each region j and each meteorological regime k. Using these data, we calculated the RIVAD transport efficiencies $\bar{\alpha}_j^{RIV}$ by using the relationship

$$\left[\frac{\Delta SO_4}{SO_4}\right]_j^{RIV} = \bar{\alpha}_j^{RIV} \bar{\beta}_j^{RIV} \frac{\Delta E}{E} = \bar{\alpha}_j^{RIV} \frac{\Delta E}{E} \tag{11}$$

since, for RIVAD, the nonlinearity coefficient β is always equal to one. Also, we applied Equation 11 for each group of days characterized by the same meteorological regime k and, therefore, obtained the transport efficiencies α_{jk}^{RIV} using the relationship

$$\frac{(\Delta SO_4)_{jk}^{RIV}}{(SO_4)_{jk}^{RIV}} = \alpha_{jk}^{RIV} \beta_{jk}^{RIV} \frac{\Delta E}{E} = \alpha_{jk}^{RIV} \frac{\Delta E}{E}. \tag{12}$$

In an analogous way, the fractional light extinction improvements can be calculated by using either the regression method used by SAI[1], which establishes an empirical relationship between sulfate concentration, relative humidity and light scattering, or the method of Latimer and Hogo[2], which uses the median visibility values in the eastern United States. The former method makes direct use of the noontime measurements of relative humidity, while the latter method cannot differentiate between meteorological regimes. The calculation of the light

extinction improvements allows the calculation of the RIVAD's terms $\bar{\epsilon}_j^{RIV}$ and ϵ_{jk}^{RIV}, by applying

$$\overline{\left[\frac{\Delta LE}{LE}\right]}_j^{RIV} = \bar{\epsilon}_j^{RIV} \overline{\left[\frac{\Delta SO_4}{SO_4}\right]}_j^{RIV} \tag{13}$$

and

$$\frac{(\Delta LE)_{jk}^{RIV}}{(LE)_{jk}^{RIV}} = \epsilon_{jk}^{RIV} \frac{(\Delta SO_4)_{jk}^{RIV}}{(SO_4)_{jk}^{RIV}} \tag{14}$$

Intercomparison Results

The Average Regional Transport Efficiencies $\bar{\alpha}_j$

The eight "regional" values $\bar{\alpha}_j^{REL}$ (j = 1, 2, ... 8) are presented in Table I. As discussed in Section 3, these values allow a "bulk" comparison with the α_{jk} values that were computed by Zannetti et al.[4] in a sample application of the semiempirical methodology. The latter α_{jk} values, which we denote here by α_{jk}^{AV}, were computed for every region j and every meteorological regime k. Therefore, the equivalent $\bar{\alpha}_j^{AV}$ are

$$\bar{\alpha}_j^{AV} = \sum_k p_{jk}\, \alpha_{jk}^{AV} \tag{15}$$

where p_{jk} is the relative frequency of occurrence in 1980 of the meteorological regime k in the region j. We calculated p_{jk} from our meteorological classification without including (as we had in previous analyses) a special class for days characterized by relative humidity greater than 85 percent. This is necessary because RELMAP simulations include all days of the year and, in this comparison of α values, we had to be consistent in our assumptions. The $\bar{\alpha}_j^{AV}$ values computed by Equation 15 are presented in Table I.

The results presented in the EPA's RIA allow an approximate calculation of the $\bar{\alpha}_j$ values associated with the transfer matrices of the ASTRAP model ($\bar{\alpha}_j^{AST}$), the MONTE CARLO model ($\bar{\alpha}_j^{MC}$) and the RIA's final calculations ($\bar{\alpha}_j^{RIA}$, i.e., the average of $\bar{\alpha}_j^{AST}$ and $\bar{\alpha}_j^{MC}$). In fact, by averaging simulated sulfate values over each region j (with no distinction between urban and rural), we obtained $\overline{[SO_4^{2-}]}_j^{(old)}$ and $\overline{[SO_4^{2-}]}_j^{(new)}$ values. These allowed the calculation of $\bar{\alpha}_j^{AST}$, $\bar{\alpha}_j^{MC}$ and $\bar{\alpha}_j^{RIA}$ using the relationship

$$\bar{\alpha}_j = \frac{\overline{[SO_4^{2-}]}_j^{(new)} - \overline{[SO_4^{2-}]}_j^{(old)}}{\overline{[SO_4^{2-}]}_j^{(old)}} \cdot \frac{E}{\Delta E} \tag{16}$$

where, in this case, the total fractional control associated with the SO_2 control scenario (the "0.25 ppm 1-hour alternative NAAQS" scenario) is $\Delta E/E = -0.43$.[4] The values $\bar{\alpha}_j^{AST}$, $\bar{\alpha}_j^{MC}$ and $\bar{\alpha}_j^{RIA}$, computed by Equation 16 are presented in Table I.

For this comparison, SAI ran the RIVAD model for each day of the year 1980. This allowed the calculation of the RIVAD annual average transport efficiencies $\bar{\alpha}_j^{RIV}$, which are presented in Table I. This calculation was performed using a 12-million-ton SO_2 emission reduction scenario with $\Delta E/E = -0.57$. Actually, two sets of $\bar{\alpha}_j^{RIV}$ values were

computed. The first set, which is shown in Column (A) of Table I, was computed by using all the RIVAD outputs, while the second set, in Column (B), was computed using only the SO_4^{2-} outputs calculated by RIVAD at noontime. The first set is more appropriate for comparison with the other methods, but the second set is important for establishing the appropriate relationship between sulfate concentration and visual range improvements. We note, with some surprise, that the (B) values are 10 to 20 percent lower than the (A) values, a fact that we cannot explain at this time. It is true that RIVAD uses an SO_2-to-SO_4 conversion rate that is a function of the time of day and that reaches its highest value at noon. However, because of the assumed linearity of the transformation, the efficiency terms α should not show large variations. If this difference represents a true atmospheric behavior, we can reach the important conclusion that approaches such as the transfer matrices, which provide average SO_4^{2-} improvements due to SO_2 control scenarios, overestimate by 10 to 20 percent the actual SO_4^{2-} improvements at noon, the time when visual range measurements or simulations are often made.

All the $\bar{\alpha}_j$ values discussed above are presented in Table I, which also shows the ratios of the different sets of values over $\bar{\alpha}_j^{AV}$. The highest $\bar{\alpha}_j$ values are $\bar{\alpha}_j^{REL}$, which are 15 to 50 percent higher than the $\bar{\alpha}_j^{AV}$ values. Also, the three $\bar{\alpha}_j$ values derived from the EPA's transfer matrices are generally higher than both $\bar{\alpha}_j^{AV}$ and $\bar{\alpha}_j^{RIV}$. We also note that the $\bar{\alpha}_j^{AV}$ values in Table I are not "extreme" values. In other words, with the exception of the CC region, where the $\bar{\alpha}_j^{AV}$ values are indeed the lowest, they are generally within the range of variation of the other $\bar{\alpha}_j$ values.

If we consider all the uncertainties in the different technical approaches that are compared in Table I, we should not be surprised at the differences in the tabulated $\bar{\alpha}_j$ values. It may appear that the $\bar{\alpha}_j$ values that were derived from the application of the transfer matrices and RIVAD are more "objective" than the more subjectively derived $\bar{\alpha}_j^{AV}$. In reality, the correct calculation of the transport efficiencies represented by α requires a precise description of atmospheric transport patterns, which is provided neither by current dispersion models nor by the semiempirical approach. Although the transfer matrices were computed from simulations performed by Lagrangian models that take into account many of the complexities of atmospheric transport, uncertainties in air mass trajectory evaluation are still large due to inadequate input data and numerical simplifications such as the model's inability to account for wind speed and direction shear.

The recent results by Policastro[8], showing poor correlation between tracer concentrations and concentrations predicted by eight short-term long-range transport models, suggest skepticism concerning the performance one can expect from models such as RELMAP, ASTRAP, MONTE CARLO and RIVAD. As long as plume trajectory direction uncertainties remain in the range of 20 to 45 degrees, the evaluation of α by deterministic models remains questionable. We conclude, therefore, that we have no solid reasons, at present, to prefer other $\bar{\alpha}_j$ values over the $\bar{\alpha}_j^{AV}$ values, but rather that the above results represent different sets of information concerning possible values for $\bar{\alpha}_j$.

The Terms ϵ_{jk}

As shown in Equation 7, the terms $\epsilon_{jk}^{(w)} = \gamma_{jk}^{(w)} \delta_{jk}^{(2)}$ relate the fractional improvements in light extinction to the fractional improvements of the concentration of fine sulfates. A set of $\gamma_{jk}^{(w)}$ and $\delta_{jk}^{(w)}$ values for each region j and meteorological regime k was computed by Zannetti et al.[3] and their products ϵ_{jk}^{AV} are presented in Table II.

As we discussed earlier, the EPA used a simplified approach to estimate the visibility changes expected from the changes in sulfate concentrations predicted by the transfer matrix approach. We showed that this method corresponds to a choice of a fixed $\epsilon^{(w)}$ value equal to 0.44, a value that we will refer to as ϵ^{TM}. If we compare ϵ^{TM} with the ϵ_{jk}^{AV} terms in Table II, we notice that ϵ^{TM} is larger than almost all of the ϵ_{jk}^{AV} values. Table III presents the ratios between ϵ^{TM} and ϵ_{jk}^{AV}. These ratios vary from 2.10 (i.e., ϵ^{TM} 110 percent higher than ϵ_{jk}^{AV}) to 0.95 (i.e., ϵ^{TM} 5 percent lower than ϵ_{jk}^{AV}). This means that, for the same sulfate concentration improvements, the visual range improvements computed by the transfer matrix approach are much larger, for almost all j and k, than those computed by AV's semiempirical method.

If we compare the theoretical basis behind the calculations of ϵ_{jk}^{AV} and ϵ^{TM} and the evidence provided by the limited amount of available data, the estimates ϵ_{jk}^{AV} seem more reliable than ϵ^{TM}. The calculation of ϵ^{TM} is based on the assumption that the sulfate contribution to light extinction is always 44 percent of the total, for all eastern United States regions and under all meteorological conditions. Our semiempirical analysis example, using available measurements of the sulfate fraction of fine particle mass in the eastern United States and performing a linear regression between visual range measurements and fine particle concentrations, obtained lower ϵ_{jk}^{AV} values. Only limited data were available for evaluating ϵ_{jk}^{AV}, however. We note that the uncertainties in the estimation of both ϵ_{jk}^{AV} and ϵ^{TM} are quite high.

As discussed above, RIVAD simulations allowed the calculation of $\bar{\epsilon}_j^{RIV}$ and ϵ_{jk}^{RIV} that can be compared with AV's values $\bar{\epsilon}_j^{AV}$ and ϵ_{jk}^{AV}, and with EPA's ϵ^{TM}. The values $\bar{\epsilon}_j^{AV}$ were computed in a way similar to the calculation of $\bar{\alpha}_j^{AV}$ by Equation 15, i.e.,

$$\bar{\epsilon}_j^{AV} = \sum_k p_{jk}\ \epsilon_{jk}^{AV} \qquad (17)$$

where p_{jk}, again, does not include the special class we normally use for high humidity days, to maintain consistency in the intercomparison.

The values of $\bar{\epsilon}_j^{AV}$, $\bar{\epsilon}_j^{RIV}$ and their ratios are presented in Table IV. The first set (A) was computed using the annual average SO_4^{2-} improvements and the light extinction improvements calculated according to the method of Latimer and Hogo[2], which uses average regional values of the median visual range. The second set (B) was computed using the average noontime SO_4^{2-} improvements and the light extinction improvements calculated with the regression method[3]. In spite of the shortcomings of the regression calculations, the second method is probably more reliable than the first since it uses noontime values and incorporates the measurements of relative humidity in its calculations. Moreover, the first method is strongly dependent upon the estimate of the median visual range, an estimate that is appropriate only for typical average conditions, but not for all the meteorological scenarios.

Set (A) of Table IV presents values of $\bar{\epsilon}_j^{RIV}$ that are generally lower than $\bar{\epsilon}_j^{AV}$, while Set (B) is generally higher, with the exception of the SC region. We are not able, at present, to fully explain this difference. These results, however, seem to suggest that the choice of $\epsilon^{TM} = 0.44$ throughout the entire eastern United States is probably too high. Also, we note that, while the $\bar{\epsilon}_j^{AV}$ values do not vary much from region to region, the $\bar{\epsilon}_j^{RIV}$ values possess a large regional variation that, at the present time, cannot be explained.

Conclusions

We have compared AV's semiempirical approach, the EPA's transfer matrix approach and the RIVAD model under similar conditions and using the same 1980 meteorological input. We find the following:

1. The transport efficiencies (α terms) of the EPA's transfer matrices (especially those based on the RELMAP model) are mostly higher than AV's. The EPA's α values generate light extinction improvements that, in comparison with AV's, are 15 to 50 percent higher (using $\bar{\alpha}_j^{REL}$, based on the RELMAP model), 6 to 37 percent higher (using $\bar{\alpha}_j^{AST}$, based on the ASTRAP model), 4 percent lower to 23 percent higher (using $\bar{\alpha}_j^{MC}$, based on the MONTE CARLO model), and 3 to 30 percent higher (using $\bar{\alpha}_j^{RIA}$, the average of $\bar{\alpha}_j^{AST}$ and $\bar{\alpha}_j^{MC}$). RIVAD transport efficiencies α are, instead, very similar to to AV's. We have no clear evidence, at present, for preferring one approach over the other.
2. The EPA's and RIVAD's approaches use a linear SO_2-to-SO_4^{2-} transformation, while AV has included nonlinearity. (The RIVAD modeling of Latimer and Hogo[2] did consider nonlinearity, however.) We believe that an estimate of nonlinearity should be included. By not including this term, light extinction improvements are probably overestimated by 0 to 43 percent, versus those which would occur if nonlinearity exists.
3. The simple methodology used in the RIA for computing ϵ^{TM} probably overestimates, in most cases, the light extinction improvements. The comparison with AV's approach, based on some limited measurements, shows that ϵ^{TM} is 5 percent lower to 110 percent higher than the ϵ_{jk}^{AV} values. The efficiencies ϵ computed by RIVAD are relatively similar to AV's, even though the ϵ^{RIV} terms possess large, unexplained regional variations (see Table IV).
4. The RIA's calculation of annual visual range improvements does not take into account the effects of those days in which visibility is impaired by natural weather conditions and, therefore, on which visibility cannot be improved by ameliorating air pollution. The comparison with AV's approach, which accounts for days with relative humidity higher than 85 percent, shows that this omission by the EPA should cause the transfer matrix method to overestimate the light extinction improvements by at least 5 to 7 percent. Similarly, RIVAD runs exclude days with high relative humidity (i.e., RH > 85 percent). This causes the RIVAD method to overestimate the annual light extinction improvements by at least 5 to 7 percent.

The combination of the four factors above causes major differences between the visual range improvements computed by the different approaches. In fact, the EPA's TM improvements are typically larger than AV's by a factor of two.

Acknowledgments

We thank Mr. Henry Hogo of Systems Applications, Inc. (SAI) for his technical support and his running of the RIVAD model. Appreciation is extended to Mr. Terry Clark, of the U.S. Environmental Protection Agency (EPA), who provided us with a recently updated version of the RELMAP transfer matrices. We appreciate the help

provided by Dr. Chris Pilinis in finalizing the manuscript, Ms. Wendy Webb for preparing the manuscript and Ms. Anita Spiess for editorial review.

This study was sponsored by the Utility Air Regulatory Group (UARG).

References

1. SAI, ***Visibility and other air quality benefits of sulfur dioxide emission controls in the eastern United States***, Systems Application Inc. Report SYSAPP-84/165, San Rafael, CA, 1984.
2. D.A. Latimer and H. Hogo, "The relationship between SO_2 emissions and regional visibility in the eastern United States," In: ***Visibility Protection: Research and Policy Aspects***, P.S. Bhardawja, Editor, APCA, Pittsburgh, PA, 1987.
3. U.S. Environmental Protection Agency, ***Regulatory impact analysis on the National Ambient Air Quality Standards for sulfur oxides (sulfur dioxide)***, Draft Report prepared by EPA Air Quality Management Division, Office of Air and Radiation, Research Triangle Park, NC, 1986, revised in 1988.
4. P. Zannetti, I. Tombach, and S. Cvencek, ***Semi-empirical analysis of the visibility improvements from SO_2 emission controls in the eastern United States***, AeroVironment Report AV-FR-87/599R, Monrovia, CA, 1987.
5. P. Zannetti, I. Tombach, and S. Cvencek, "Semi-empirical analysis of the visibility improvements from SO_2 emission controls in the eastern United States," ***Proceedings***, 81st Annual APCA Meeting. Dallas, TX, 1988.
6. B.L. Niemann, Regional acid deposition calculations with the IBM PC LOTUS 1-2-3 System, ***Environ. Software, 1***, 175, 1986.
7. J. Bachmann, "Calculation of visual range changes from predicted sulfate changes," Memorandum to Tom Walton, June 10, 1985.
8. A.J. Policastro, M. Wastag, L. Coke, R.A. Carhart, and W.E. Dunn, ***Evaluation of short-term long-range transport models; Volume 1, Analysis procedures and results***, EPA Document EPA-450/4-86-016a, Research Triangle Park, NC, 1986.

Table I. Comparison of "regional" α values, using AV's semiempirical approach, EPA's transfer matrix, and the RIVAD model.

j	Region	$\bar{\alpha}_j^{AV}$	$\bar{\alpha}_j^{REL}$	$\frac{\bar{\alpha}_j^{REL}}{\bar{\alpha}_j^{AV}}$	$\bar{\alpha}_j^{AST}$	$\frac{\bar{\alpha}_j^{AST}}{\bar{\alpha}_j^{AV}}$	$\bar{\alpha}_j^{MC}$	$\frac{\bar{\alpha}_j^{MC}}{\bar{\alpha}_j^{AV}}$	$\bar{\alpha}_j^{RIA}$	$\frac{\bar{\alpha}_j^{RIA}}{\bar{\alpha}_j^{AV}}$	$\bar{\alpha}_j^{RIV}$	$\frac{\bar{\alpha}_j^{RIV}}{\bar{\alpha}_j^{AV}}$	(A) $\bar{\alpha}_j^{RIV}$	(A) $\frac{\bar{\alpha}_j^{RIV}}{\bar{\alpha}_j^{AV}}$	(B) $\bar{\alpha}_j^{RIV}$	(B) $\frac{\bar{\alpha}_j^{RIV}}{\bar{\alpha}_j^{AV}}$
1	NE urban	0.72	0.86	1.19	0.79	1.10	0.69	0.96	0.74	1.03	0.77	1.07	0.83	1.15	0.70	0.98
2	NE rural	0.72	0.83	1.15	0.79	1.10	0.69	0.96	0.74	1.03	0.75	1.04	0.81	1.12	0.68	0.94
3	NC urban	0.86	1.04	1.21	0.91	1.06	0.86	1.00	0.89	1.03	0.73	0.85	0.78	0.91	0.79	0.92
4	NC rural	0.86	1.04	1.22	0.91	1.06	0.86	1.00	0.89	1.03	0.73	0.85	0.76	0.89	0.79	0.92
5	CC urban	0.69	0.98	1.42	0.94	1.37	0.85	1.23	0.90	1.30	0.89	1.29	0.90	1.30	0.79	1.14
6	CC rural	0.69	1.03	1.50	0.94	1.37	0.85	1.23	0.90	1.30	0.87	1.26	0.88	1.28	0.77	1.12
7	SC urban	0.69	0.92	1.34	0.83	1.21	0.82	1.19	0.82	1.20	0.68	0.99	0.68	0.99	0.61	0.89
8	SC rural	0.69	0.90	1.31	0.83	1.21	0.82	1.19	0.82	1.20	0.63	0.92	0.64	0.94	0.59	0.86

NE = Pennsylvania and northeastward
CC = Coastal states from Delaware to South Carolina
NC = The Midwest
SC = Tennessee and southward

Table II. The terms ϵ_{jk}^{AV} computed with the semiempirical approach.

j	Region	k = 1 cPk	k = 2 cPw	k = 3 mT	k = 4 Tr	k = 5 cT	k = 6 cP2	k = 7 mP
1	NE urban	0.21	0.23	0.32	0.26	0.21	0.28	0.33
2	NE rural	0.27	0.27	0.37	0.30	0.29	0.28	0.37
3	NC urban	0.27	0.24	0.38	0.25	0.27	0.20	0.45
4	NC rural	0.27	0.25	0.39	0.29	0.27	0.24	0.47
5	CC urban	0.25	0.25	0.29	0.28	0.26	0.25	0.25
6	CC rural	0.31	0.37	0.41	0.34	0.33	0.31	0.34
7	SC urban	0.25	0.23	0.32	0.34	0.23	0.22	0.33
8	SC rural	0.26	0.37	0.39	0.38	0.27	0.26	0.42

Table III. Ratio of EPA's ϵ^{TM} to AV's ϵ_{jk}^{AV}.

j	Region	k = 1 cPk	k = 2 cPw	k = 3 mT	k = 4 Tr	k = 5 cT	k = 6 cP2	k = 7 mP
1	NE urban	2.10	1.96	1.37	1.72	2.07	1.56	1.36
2	NE rural	1.66	1.66	1.23	1.49	1.56	1.56	1.19
3	NC urban	1.64	1.89	1.18	1.78	1.66	2.18	0.99
4	NC rural	1.64	1.77	1.13	1.51	1.66	1.85	0.95
5	CC urban	1.76	1.76	1.54	1.60	1.73	1.76	1.75
6	CC rural	1.44	1.19	1.08	1.31	1.36	1.44	1.33
7	SC urban	1.79	1.96	1.40	1.29	1.90	2.00	1.34
8	SC rural	1.72	1.20	1.13	1.17	1.63	1.70	1.07

Table IV. Comparison of $\bar{\epsilon}_j^{RIV}$ versus $\bar{\epsilon}_j^{AV}$.

j	Region	$\bar{\epsilon}_j^{AV}$	$\bar{\epsilon}_j^{RIV}$	(A) $\frac{\bar{\epsilon}_j^{RIV}}{\bar{\epsilon}_j^{AV}}$	$\bar{\epsilon}_j^{RIV}$	(B) $\frac{\bar{\epsilon}_j^{RIV}}{\bar{\epsilon}_j^{AV}}$
1	NE urban	0.25	0.27	1.08	0.41	1.64
2	NE rural	0.29	0.26	0.92	0.39	1.34
3	NC urban	0.27	0.21	0.79	0.45	1.67
4	NC rural	0.28	0.21	0.73	0.43	1.54
5	CC urban	0.25	0.19	0.78	0.34	1.36
6	CC rural	0.33	0.18	0.56	0.31	0.94
7	SC urban	0.29	0.17	0.59	0.22	0.76
8	SC rural	0.35	0.17	0.48	0.22	0.63

RELATIONSHIP OF TRENDS IN REGIONAL SULFUR DIOXIDE EMISSIONS TO PARTICULATE SULFATE CONCENTRATIONS IN THE SOUTHWESTERN UNITED STATES

James F. Sisler
Cooperative Institute for Research in the Atmosphere
Colorado State University
Fort Collins, CO

William C. Malm
National Park Service, Air Quality Division
Fort Collins, CO

Abstract

A large component of atmospheric light extinction is due to fine ammonium sulfate aerosol, a byproduct of sulfur dioxide emissions. Large variations in sulfur dioxide emissions from copper smelters in the last decade have provided an opportunity to study the relationship between sulfur dioxide emissions and ammonium sulfate concentrations at various receptor sites. A particular point of interest is the extent to which changes in sulfur dioxide emissions are reflected as changes in ammonium sulfate concentrations. Using a relationship between fine ammonium sulfate concentrations and atmospheric extinction, the impact of controlling emissions on visibility may be examined. To this end, data from the National Park Service particulate monitoring network has been synchronized in time with monthly and seasonal averages of smelter emissions. Empirical results show a relationship between smelter emissions and particulate sulfate concentrations at three sites, Grand Canyon National Park, Tonto National Monument, and Chiricahua National Monument.

Introduction

The relation between changes in emissions of sulfur dioxide (SO_2) and ammonium sulfate aerosol in the Southwestern United States has been investigated during the last several years[1,2]. Empirical models have been developed that examine source-receptor relationships between SO_2 emissions and sulfate concentrations[3,4]. Due to emissions from other anthropogenic sources and meterological variability, isolation of the effect of one source or source area on a particular receptor is difficult. Efforts to overcome such difficulties have utilized extensive data bases of aerosol concentrations at various receptors, emission inventories, and meterological data. Many methods used to identify sources of anthropogenic precursors to atmospheric sulfate have involved the use of back trajectories of air parcels arriving at receptors[5,6].